Optimization of both Operating Costs and Energy Efficiency in the Alumina Evaporation Process by a Multi-Objective State Transition Algorithm

Yalin Wang,* Haiming He, Xiaojun Zhou, Chunhua Yang and Yongfang Xie

College of Information Science and Engineering, Central South University, Changsha, 410083, Hunan, China

The alumina evaporation process (AEP) is an indispensable step for the reuse of sodium aluminate solution by evaporating excess water contained in the solution. The selection of optimal operating parameters is a complicated task because the process is influenced by many nonlinear factors when both the quality and quantity of the product are concerned. In this paper, we formulate a multi-objective optimization model to maintain the balance of operating costs and energy efficiency in AEP, and a multi-objective state transition algorithm (MOSTA) is proposed for solving this problem. With the aim of solving the constrained multi-objective problem, a search archive strategy of elite populations and a novel infeasible solution replacement mechanism are integrated into STA. Some infeasible solutions with better performances are allowed to be saved and participate randomly in the evolution to select optimal solutions from all possible directions. A mutation operator is introduced into the evolutionary process to enhance the global search ability. Simulation results from some benchmark test problems show that the proposed method tends to converge quickly and effectively to the true Pareto frontier with better distribution. The proposed algorithm is successfully applied to solve the multi-objective optimization problem arising in AEP. The optimal results show that operating costs and energy loss are considerably reduced, by approximately 13.63 % and 13.39 %, respectively.

Keywords: alumina evaporation process, multi-objective optimization, STA, Pareto archive strategy

INTRODUCTION

The alumina production process[1,2] includes dissolving aluminum-bearing minerals in a caustic soda solution to prepare a sodium aluminate solution. Aluminum hydroxide is obtained from the sodium aluminate solution by decomposition, and then filtered and roasted to obtain alumina. The remaining mother liquor from the filtration process needs to be evaporated and reused to dissolve a batch of new aluminum-bearing minerals. The alumina evaporation process (AEP) is an indispensable step in which excess water is evaporated with the help of high-temperature and high-pressure steam. To keep the solution concentration in balance, adequate energy (i.e., live steam) must be continually supplied. A total of 22.47 % of the energy in the whole alumina production process is consumed in the evaporation process.[3] Therefore, there exists industrial significance in achieving operational optimization in the evaporation process to reduce the cost of live steam consumption, improve energy efficiency, and ensure the quality of the outlet mother liquor.

The AEP is an energy-intensive process with complex energy efficiency relations and many interacting factors.[2] There exists strong coupling between the mother liquor and the vapour steam from the multiple-effect evaporators. The production costs and energy utilization of AEP are affected by the temperature, concentration, and quantity of the mother liquor and by the temperature and pressure of the live steam at both the inlet and outlet of the evaporators. Ji[4] studied the influence of different operating parameters on evaporation plant sub-models, with the main objective of minimizing plant energy costs. Khanam[5] studied the effect of operating parameters on the steam consumption per tonne of evaporated water (SCPTEW), and a mixed integer nonlinear programming model was presented to schedule production and cleaning operations in a sugar plant with performance decay.[6] Chai[7] established a mathematical model of an evaporation system using a state-space formulation with multiple time delays, and optimized the SCPTEW using particle swarm optimization (PSO),[2] where the objective is to find a control law such that the specific quality of the mother liquor is met with the least energy usage, and the constraints imposed on the state and the control are satisfied. Although the optimization of AEP has enabled energy-saving or cost-saving techniques, it does not take into account operating costs and energy efficiency simultaneously, which can lead to unreasonable usage of high-quality energy or inadequate production capacity. To solve these problems, the optimization of both operating costs and energy efficiency in AEP is necessary.

The optimization problem in AEP is subject to the concentration of the outlet solution, production capacity, and other process requirements. The operating parameters to be optimized, such as the pressure and flow rate of the live steam as well as the temperature and flow rate of the feed mother liquor, have complex nonlinear relationships with the optimization objects and constraints, which lead to a narrow feasible solution space. Therefore, this is a challenging issue for solving the complex optimization problem with constraints (CMOP) in AEP. It is essential to find an effective method to find a set of optimal operating parameters satisfying the production requirements.

As a heuristic search paradigm, evolutionary algorithms (EAs) maintain a population of potential solutions to achieve the global

* *Author to whom correspondence may be addressed.*
E-mail address: ylwang@csu.edu.cn
Can. J. Chem. Eng. 94:53–65, 2016

DOI 10.1002/cjce.22353
Published online 16 November 2015 in Wiley Online Library (wileyonlinelibrary.com).

search, and this approach has numerous advantages in finding the Pareto optimal set for multi-objective optimization problems (MOPs). Since the pioneering attempt of Schaffer to solve MOPs,[8] many types of multi-objective evolutionary algorithms (MOEAs) have been proposed and widely used in different applications.[9–10] Based on different selection mechanisms, Coello[11] classified MOEAs into three categories: aggregating functions, population-based approaches, and Pareto-based approaches. The aggregating functions combine multiple objectives into a single scalar value.[12–13] By repeating the evolutionary process for a given number of iterations with different settings of the aggregating function, the whole trade-off surface can be obtained.[14] However, the difficulty of selecting the appropriate weight for each objective remains its main disadvantage. The population-based approaches attempt to separate multiple objectives during the evolution by diversifying the search. A number of sub-populations are generated by performing proportional selection for each objective function in turn. The main disadvantage of this approach is that it cannot be directly incorporated into the selection process of the algorithm.[11] Most MOEAs are Pareto-based approaches, which incorporate the Pareto optimality into their selection mechanism. The representative methods of this approach have the rank-based fitness assignment method of genetic algorithms,[15] the niched Pareto genetic algorithm (NPGA),[16] the non-dominated ranking genetic algorithm (NSGA)[17] and its classical improved version NSGA-II,[18] the micro-genetic algorithm,[19] the Pareto archive evolution strategy (PAES),[20] the strength Pareto evolutionary algorithm (SPEA)[21] and its improved version SPEA2,[22] the incremental multi-objective evolutionary algorithm (MOEA),[23] and the MOEA based on decomposition techniques.[24–25]

In addition to the traditional EAs, other evolutionary meta-heuristics have also been proposed and used to successfully solve the MOPs, such as Scatter Search (SS),[26–27] Particle Swarm Optimization (PSO),[28–30] Differential Evolution (DE),[31–33] and others. By combining different ideas or meta-heuristics, the proposed algorithm may further improve the effectiveness of methods in order to overcome the inherent limitations of a single evolutionary algorithm or meta-heuristic. Nebro[27] proposed a hybrid scatter search for MOPs which combines the archive strategy, mutation operators, and crossover operators from evolutionary algorithms to find the Pareto frontier. Coello[28] also incorporated the external population by the mechanism of adaptive mesh into the multi-objective particle swarm optimization, which presented a new particle update strategy through the mutation of the particle itself and the search range. The mutation scale of the particle is proportional to the population size to avoid premature convergence and to maintain diversity. Computational results showed that the MOPSO is very competitive with the MOPs.

Conversely, with the significant growth of using EAs for constrained optimization problems (COPs) in recent decades, many different constraint handling techniques have been proposed.[34–37] Michalewicz and Schoenauer[34] classified constraint handling techniques by EAs into four categories: preserving the feasibility of solutions, penalty functions, separating feasible from infeasible solutions, and hybrid methods. These methods differ in how to handle infeasible individuals throughout the search process. The penalty function method is the most widely used, but it strongly depends on the selection of the penalty parameters. To address this limitation, some novel methods are proposed based on the preference of feasible and infeasible solutions. Deb[38] proposed a tournament selection operator to devise a penalty function approach that does not require any penalty parameter. Mezura-Montes and Coelle[39] presented a simple multi-membered evolution strategy. The approach uses a simple diversity mechanism to allow infeasible solutions to remain at a certain probability in the population, which ensures that it can quickly find the global optimal solution in a reasonably feasible region of the search space.

Although the MOPs and constraint handling techniques have received much attention, the CMOPs are still challenging in practice when considering the constraints of the technological process. Wang[32] designed a hybrid DE algorithm using the simplex method (SM-DEMO) for bauxite grinding-classification operation. The proposed algorithm is formed by combining the simplex method and an elite population mechanism to ensure that some infeasible solutions with better performances are allowed to take part in the evolutionary process. The mechanism of the functionally partition is intended to find an optimal solution from all possible directions.

Inspired by the successful search strategies and constraint handling techniques applied in previous research, in this paper, based on the specific industrial background of AEP, we establish a multi-objective optimization model to ensure the best performance of the operating parameters in AEP, and a multi-objective state transition algorithm (MOSTA) is proposed for solving real-world MOPs. Based on its special operators, the basic STA has better performance for solving high-dimensional and nonlinear single objective optimization problems compared with classical GA and PSO. As a result, we extend this algorithm to solve the multi-objective optimization problem arising in AEP. The main contributions and novelty of this paper can be summarized as follows: Firstly, we introduce a novel stochastic optimization algorithm, the state transition algorithm (STA),[40] in which the four special operators, including rotation, translation, expansion, and axesion, are designed for the requirements of solving continuous optimization problems concerning global and local searches. Second, apart from using STA as the search engine, MOSTA also presents a search archive strategy based on Pareto non-dominated ranking of the elite population to select optimal solutions in a candidate set, and it introduces a new state transition operator and mutation operator to enhance the global search ability and maintain the diversity of the solution candidates. Experimental results have demonstrated the effectiveness of the proposed algorithm. Finally, MOSTA is successfully applied to the optimization of AEP by combining a novel infeasible solution replacement mechanism with multi-objective optimization. To the best of our knowledge, this is the first time that a multi-objective version of STA is proposed and applied to continuous MOPs.

OPTIMIZATION MODEL OF THE AEP

Alumina Evaporation Process

A typical industrial AEP, which transfers the heat of high-temperature and high-pressure steam to a sodium aluminate solution to remove excess water by using an evaporator and other heat transfer devices, is shown in Figures 1–2.

The process consists of four falling film tube evaporators, three direct pre-heaters, and three flash evaporators.[2] The feed mother liquor discharged from the filtration process is pumped to the IIIrd and IVth evaporators through a feeding pump, and the output liquid coming from the IVth evaporator is pumped into the IIIrd pre-heater and then goes into the IIIrd evaporator after being heated close to its boiling point. In the same way, the feed mother liquid goes into the IInd and Ist evaporators in sequence, and then the liquor coming from the Ist evaporator is pumped into the 1st,

Figure 1. The evaporators in AEP.

2nd, and 3rd flash evaporators in sequence because of the differential pressure. Finally, the final mother liquor is output through pumping. The new steam first passes into the Ist evaporator, and then vapour coming from the different evaporators is pumped into the next evaporator. Vapour coming from the 1st, 2nd, and 3rd flash evaporators is pumped into the Ist, IInd, and IIIrd evaporators, respectively. Vapour evaporated by the condensate tanks is pumped into the evaporator for re-utilization.

As described in the Introduction section, the optimization objective of AEP is to fully use the current device's handling ability to control the pressure and flow rate of the live steam and the temperature and flow rate of the feed mother liquor, and to regulate the temperature distribution of the process to satisfy the concentration requirements of the final mother liquor and to minimize both operating costs and energy loss efficiency. Although energy-saving equipment such as flash evaporators and pre-heaters can be added to reduce steam consumption, they are not always helpful. The reason why these energy-saving devices fail is mainly due to operator error. This leads to problems such as unqualified mother liquor, excessive live steam consumption, and low energy efficiency when applied in an actual industrial process. Therefore, it is necessary to establish an optimization model for the effective regulation of operating parameters in AEP.

Optimization Model of AEP based on the Exergy Evaluation Index

Although the optimization problem of AEP has received much attention, the existing solutions do not simultaneously take into account the operating costs and energy efficiency. Optimizing both of these can bring higher economic benefits in the actual evaporation process. Thus, in this section, we build a multi-objective optimization model of AEP by introducing the exergy evaluation index into the optimization model of Zhu.[2] The definitions of the indices, decision variables, and parameters are listed in the Nomenclature section. These definitions will be used for the model of the AEP.

Considering the exchange of energy and material from the mother liquor and the steam flow, the AEP can be treated as a steady-flow open system that satisfies a balance of material and energy. Based on the material and mass balance principles, the mass of solute input into the i^{th} unit equals the mass of solute going out of the i^{th} unit. Thus, the formula of the material balance is described as follows:[2]

$$F_i C_i^j = (F_0 + F_{01}) C_0^j,\ i = 1,...,6,\ j = 1,2,3 \tag{1}$$

$$F_7 C_7^j = F_0 C_0^j,\ j = 1,2,3 \tag{2}$$

$$F_i = \phi_i\,(Q_i,\ \rho_i, T_i, T_r, cp_i, H_i),\ i = 1,...,7 \tag{3}$$

where $\phi_i(\cdot)$ represents the i^{th} function relationship between F_i and the operating variables (for a detailed description, see Equations (1–5) in the optimization model of Zhu[2]). Based on the data collected from a whole-acid cycle of AEP under different scarring conditions at the

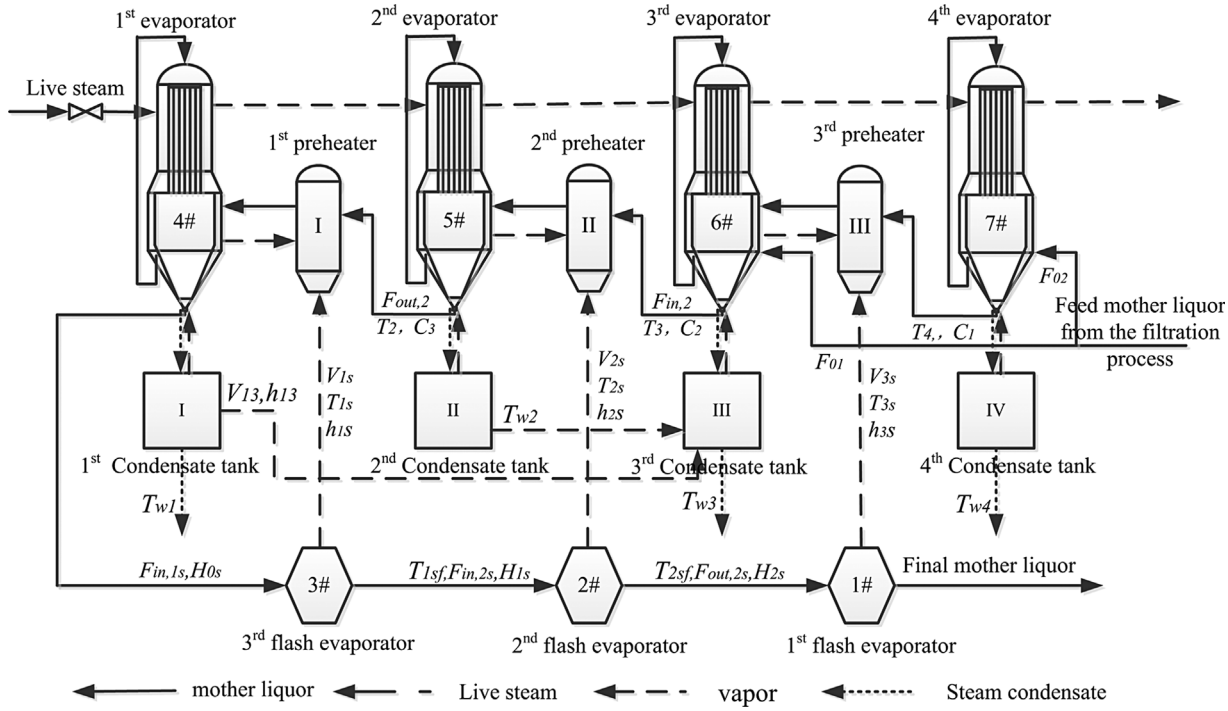

Figure 2. Flow schematic of an AEP.

China Aluminum Corporation, ρ_i, cp_i, h_i, H_i, and T_{ni} were determined by a regression method. Their definitions are as follows:

$$cp_i = 4.18 - \frac{(2.994C_i^1 + 2.923C_i^2 + 3.266C_i^3)}{\rho_i},\ i = 0,...,7 \tag{4}$$

$$\rho_i = 1045 + 0.8C_i^3 + 1.2C_i^2 + 0.8C_i^1,\ i = 0,...,7 \tag{5}$$

$$h_i = H_i - 4.18(T_{ni} - T_r),\ i = 0,...,7 \tag{6}$$

$$H_i = 2019.4 + 1.741T_{ni} - 0.002\,128\,(T_{ni} - T_r)^2,\ i = 0,...,7 \tag{7}$$

$$T_{ni} = 0.77P_i + 282.68P_i^{0.064} + 81.22P_i^{0.3037} + 262.1 \tag{8}$$

Exergy is a physical quantity that describes both energy quality and quantity, and it represents the ability to transform energy into useful work. Considering the strong coupling between the mother liquor and the steam flow and multi-heat sources from each unit in the AEP, the energy balance of the AEP system can be regarded as the combination of a series of exergy balance models based on the energy flow direction.

In general, the formula of the exergy balance is described as follows.

$$Ex_{in1} - Ex_{out1} = (Ex_{out2} - Ex_{in2}) + \eta_e \tag{9}$$

where η_e is the loss of exergy in AEP. We can see that the exergy of the cool fluid can increase from Ex_{in2} to Ex_{out2}, and the exergy of the thermal fluid can decrease from Ex_{in1} to Ex_{out1}. Hence, the exergy balance model of each unit has the following equations.

(1) The exergy balance equations of the flash evaporators from units #1–3 are shown as follows:

$$E_{Ti} = F_{i+1}\,\rho_{i+1}\,e_{mi+1} = V_i\,e_{vi} + F_i\rho_i\,e_{mi} + \eta_{e,Ti},\ (i = 1,2,3) \tag{10}$$

where E_{Ti} is the total exergy input into the i^{th} unit, and η_i is the loss of exergy from the i^{th} unit.

(2) The exergy balance equations of the pre-heaters from units #4–7 are shown as follows:

$$\begin{aligned} E_{pT_i} &= F_{i+1}\,\rho_{i+1}\,e_{mi+1} + V_{7-i}\,e_{v(7-i)} + V_{pi}e_{vi} \\ &= (F_{i+1}\rho_{i+1} + V_{7-i} + V_{pi})e_{mpi} + \eta_{e,pTi},\ (i = 4,5,6,7) \end{aligned} \tag{11}$$

where E_{pTi} is the total exergy input into the i^{th} unit, and η_{pi} is the loss of exergy from the i^{th} unit.

(3) The exergy balance equations of the evaporators from units #4–7 are shown as follows:

$$\begin{aligned} E_{T4} &= (F_5\rho_5 + V_3 + V_{p4})e_{mp4} + V_0e_{v0} \\ &= (V_4 + V_{p4})e_{v4} + F_4\,\rho_4\,e_{m4} + \mu_2\,V_0\,e_c \\ &\quad +(1 - \mu_2)V_0e_{n4} + \eta_{e,T4} \end{aligned} \tag{12}$$

$$\begin{aligned} E_{T5} &= (F_6\rho_6 + V_2 + V_{p5})e_{mp5} + V_4e_{v4} \\ &= (V_5 + V_{p5})e_{v5} + F_5\,\rho_5\,e_{m5} + V_4e_{n5} + \eta_{e,T5} \end{aligned} \tag{13}$$

$$\begin{aligned} E_{T6} &= (F_7\rho_7 + V_1 + V_{pi})e_{mp6} + V_5e_{v5} + \mu_2V_0e_{coi} + F_{01}\rho_0e_{m0} \\ &= (V_{p6} + V_6)e_{v6} + F_6\,\rho_6\,e_{m6} + (V_5 + \mu_2V_0)e_{n6} + \eta_{e,T6} \end{aligned} \tag{14}$$

$$E_{T7} = V_6\,e_{v6}(+F_0 - F_{01})\,\rho_0\,e_{m0} = V_7\,e_{v7} + F_7\,\rho_7e_{m7} + V_6\,e_{n7} + \eta_{e,T7} \tag{15}$$

Then, the exergy balance equation of the AEP system is shown as follows:

$$\begin{aligned} E_T &= V_0\,e_{v0} + (F_0 + F_{01}) \times \rho_0e_{m0} \\ &= F_1\,\rho_1\,e_{m1} + V_7\,e_{v7} + (1 - \mu_2) \times V_1\,e_{n4} \\ &\quad +\ V_4\,e_{n5} + (V_5 + \mu_2V_0)e_{n6} + V_6\,e_{n7} + \eta_e \end{aligned} \tag{16}$$

Here, F_1, V_i and $\mu_2\,V_0$ are obtained by a balance computation, e_{vi}, e_{ni} and e_{coi} are obtained by the Szargut environment model,[41] and e_{mi} is obtained by the IAPWS-IF97 model.[42] These parameters have the following formulas.

$$e_{coi} = (c_wT_{wi} - H_r) - T_r\,(s_{wi} - s_r);\ i = 1,2,...,7 \tag{17}$$

$$e_{ni} = (H_i - H_r) - T_{ni}\,(s_{ni} - s_r);\ i = 4,...,7 \tag{18}$$

$$e_{vi} = (H_{is} - H_r) - T_{is}\,(s_i - s_r);\ i = 0,...,7 \tag{19}$$

$$\begin{aligned} e_{mi} &= (H_i - H_r) - T_r\,(s_i - s_r) - (c_w - c_i) \\ &\quad \times \int_{T_r,p_{mi}}^{t_{mi},p_{mi}} \left(1 - \frac{T_r}{t_{mi}}\right)dT - (v_w - v_{mi})\int_{T_r,p_r}^{T_r,p_{mi}} dp \end{aligned} \tag{20}$$

Because the total exergy loss η_e of the system is absolute, we cannot compare the utilization degrees of the processes and devices under different operating conditions.[43] Thus, we use the exergy efficiency η_t of maximum utilization to replace the η_e of minimum utilization to evaluate the energy utilization degree.

As mentioned above, the optimization model in AEP has the following two objectives.

(1) The first optimization objective $f_1(x)$ is to minimize J_1, that is, the mass unit of live steam consumption per tonne of evaporated water from the mother liquor. As a main energy source, the live steam is an important indicator to measure the economic performance of AEP when the conditions of the pump power consumption are fixed. J_1 can be used to represent the operating costs of AEP, and is defined as follows.[2]

$$\min f_1(x) = \min J_1 = \frac{D_0}{W} \tag{21}$$

where W is the total water evaporated from the process, and D_0 is the total live steam required by the whole evaporation process. They are given by:

$$\begin{aligned} W &= (F_0 + F_{01})\,\rho_0 - F_1\,\rho_1 \\ &= (F_0 + F_{01})\,\rho_0 - F_1\,(1045 + 0.8C_1^3 + 1.2C_1^1 + C_1^2) \\ &= 1045\,(F_0 + F_{01} - F_1) \end{aligned} \tag{22}$$

$$\begin{aligned} D_0 &= \frac{k_1\,A_1\,\Delta t_1}{0.99\,h_0} \\ &= \frac{k_1\,A_1\,\Delta t_1}{0.99\left(3161.2 - 2.439\,T_{n0} - 0.002\,128\,(T_{n0} - T_r)^2\right)} \end{aligned} \tag{23}$$

(2) The second optimization objective $f_2(x)$ is to minimize the exergy loss efficiency. Less exergy loss efficiency means higher exergy efficiency η_t which ensures that more energy

can be used in the next process and reduces the energy consumption of the whole production process. Thus, the second optimization objective is defined as follows.

$$\min f_2(x) = 1 - \eta_t = 1 - [F_1 \rho_1 e_{m1}/(V_0 e_{v0} + F_0 \rho_0 e_{m0})] \quad (24)$$

where e_{v0}, e_{m0}, and e_{m1} are obtained by substituting $i = 0,1$ into Equations (19,20).

For an actual industry process, many operating parameters of the optimization model cannot change over a large range due to the constraints imposed by the energy balance, material balance, and production conditions, such as the required live steam pressure P_0, condenser pressure P_m, effective temperature difference of the evaporator $\Delta t_i\,(i = 4, \ldots, 7)$, flow of the feed mother liquor passing into j^{th} unit $F_{0,j}$, and concentration of the mother liquor output C_1^2. Therefore, the constraints of the optimization model are formulated as follows:

$$\begin{cases} C^2_{1,,\min} \le C_1^2 \le C^2_{1,,\max} \\ P_{0,\min} \le P_0 \le P_{0,\max} \\ P_{m,\min} \le P_m \le P_{m,\max} \\ F_{01,\min} \le F_{01} \le F_{01,\max} \\ Q_i \le k_{zi} S_i \Delta t_i \qquad i = 1, \ldots, 7 \\ \Delta t_i \ge 5 \qquad i = 4, \ldots, 7 \\ V_{i,\min} \le V_i \le V_{i,\max} \qquad i = 4, \ldots, 7 \end{cases} \quad (25)$$

where $F_{01,\min}$, $F_{01,\max}$ represent the lower and upper bounds of the feed mother liquor flow passing into the 6^{th} unit, respectively. Q_i can be calculated by the following formulas:

$$\begin{aligned} Q_4 &= (1 - \eta_{loss})[V_1 H_1 - (1 - \mu_2) V_0 T_{n4} cp_i - \mu_2 V_1 H_c] \\ Q_5 &= (1 - \eta_{loss})[V_4 H_4 - V_4 T_{n5} cp_i] \\ Q_6 &= (1 - \eta_{loss})[V_5 H_5 + \mu_2 V_1 H_c - (\mu_2 V_1 + V_5) T_{n6} cp_i] \\ Q_7 &= (1 - \eta_{loss})[V_6 H_6 - V_6 T_{n7} cp_i] \end{aligned} \quad (26)$$

In summary, the optimization problem of the AEP can be described as follows.

Based on the optimization model of AEP, we need to find a group optimal solution of decision variables $F_{01}, P_m, P_0, T_0, \Delta t_i\,(i = 4, \ldots, 7)$ so that the operating costs (Equation (21)) and the energy loss efficiency (Equation (24)) are minimized, and constraint Equations (25) are satisfied by substituting Equations (4–8) into Equations (3,17–20,26).

Now, as a typical nonlinear multi-objective optimization problem including complex equality and inequality constraints, the optimization model of AEP is hard to solve using traditional optimization methods.

CONSTRAINED MULTI-OBJECTIVE STATE TRANSITION ALGORITHM (CMOSTA)

Basic State Transition Algorithm

Resembling the concepts of state transition and state space representation in probability theory and control theory, a solution to an optimization problem is considered a state, and the process of updating the current solution is considered a state transition.

In general, the unified form of a state transition algorithm can be described as follows:[40]

$$\begin{cases} x_{k+1} = A_k x_k + B_k u_k \\ y_{k+1} = f(x_{k+1}) \end{cases} \quad (27)$$

where $x_k \in R^n$ stands for a state corresponding to a current solution to the optimization problem; $A_k \in R^{n \times n}$ and $B_k \in R^{n \times m}$ are state transition matrixes with appropriate dimensions, which are usually regarded as transformation operators for the optimization algorithm; u_k is a function of x_k and historical states; and $f(x_{k+1})$ is the objective function or evaluation function.

To solve the continuous optimization problems, four special state transformation operators are designed.[40]

Rotation transformation

$$x_{k+1} = x_k + \alpha \frac{1}{n \| x_k \|_2} R_r x_k \quad (28)$$

where α is a positive constant called the rotation factor; $R_r \in R^{n \times n}$ is a random matrix with its entries belonging to the range of $[-1,1]$; and $\| \cdot \|_2$ is the 2-norm of a vector.

Translation transformation

$$x_{k+1} = x_k + \beta R_t \frac{x_k - x_{k-1}}{\| x_k - x_{k-1} \|_2} \quad (29)$$

where β is a positive constant called the translation factor and $R_t \in R^{n \times n}$ is a random variable with its components in the range of $[0, 1]$. The translation transformation will be performed only when a better solution is found.

Expansion transformation

$$x_{k+1} = x_k + \gamma R_e x_k \quad (30)$$

where γ is a positive constant called the expansion factor and $R_a \in R^{n \times n}$ is a random diagonal matrix with its entries obeying Gaussian distribution.

Axesion transformation[44]

$$x_{k+1} = x_k + \delta R_a x_k \quad (31)$$

where δ is a positive constant called the axesion factor and $R_a \in R^{n \times n}$ is a random diagonal matrix with its elements obeying the Gaussian distribution and only one random index having a nonzero value.

The basic procedure of STA can be described in the following pseudocode:

1: **repeat**

2: **if** $\alpha < \alpha_{\min}$ **then**

3: $\alpha \leftarrow \alpha_{\max}$

4: **end if**

5: $best \leftarrow Expansion(P_S(i), SE, \beta, \gamma)$

6: $best \leftarrow Rotation(P_S(i), SE, \alpha, \beta)$

7: $best \leftarrow Axesion(P_S(i), SE, \beta, \delta)$

8: $\alpha \leftarrow \alpha / f_c$

9: **until** the specified termination criterion is met.

Here, *best* is obtained as the optimal incumbent solution by using the "greedy criterion." *SE* is the number of samples, called search enforcement. Detailed explanations of these operators can be referred to Zhu.[44]

As a stochastic optimization algorithm, compared with classical GA and PSO, the STA has better performance in terms of global search ability and convergence accuracy.[44–47] However, considering the requirements of actual AEP problems, we next propose a multi-objective STA to solve the optimization problem arising in AEP.

MOSTA Algorithm for Unconstrained MOPs

In general, a multi-objective optimization problem (MOP) can be defined as follows:

$$\begin{aligned} &\min F(X) = \min[f_1(X), f_2(X), ..., f_r(X)] \\ &\text{such that } g_i(X) \le 0;\ (i = 1, 2, ..., p) \\ &h_j(X) = 0;\ (j = p+1, ..., q) \\ &X_k \in [X_{\min}, X_{\max}];\ (k = 1, 2, ..., n) \end{aligned} \tag{32}$$

where $F(X)$ is the objective vector; $X = (x_1, x_2, ..., x_n) \in R^n$ is a decision vector; $g_i(X)$ is the i^{th} inequality constraint; $h_j(X)$ is the j^{th} equality constraint; and $X_{\min}$ and $X_{\max}$ are the lower and upper bounds of the decision variable X_k, respectively.

Next, we provide some fundamentals on Pareto optimality. Assuming $X = [x_1, x_2, ..., x_n]^T$ and $Y = [y_1, y_2, ..., y_n]^T$ are two decision vectors, X is said to dominate Y (denoted as $X \prec Y$) if and only if $f_i(X) \le f_i(Y)\ \ \forall i \in \{1, 2, ..., k\}$ and $\exists j \in \{1, 2, ..., k\}$ $f_j(X) \le f_j(Y)$. A decision vector X^* is said to be Pareto optimal if and only if there exists no X in the decision space such that $X \prec X^*$. The set of all Pareto optimal vectors is called the Pareto optimal set (denoted as P^*), and correspondingly, the set of all of the Pareto optimal objective vectors is called the Pareto frontier (denoted as PF^*), which is defined as $PF^* = \{F(X^*) | X^* \in P^*\}$

To efficiently select the true or near-optimal Pareto frontier of real-world MOPs, the proposed MOSTA is different from STA in the following three points.

Archive strategy of multi-population based on Pareto non-dominated ranking

On the basis of the above STA, many new populations are combined with the existing parent population to achieve the archive strategy of the elite population. Firstly, the size of the samples for state transition operators will be set as *SE*; another middle population for non-dominated Pareto optimality will be set as P_B; and the population for storing the Pareto optimal set will be set as P_S. The individual number of the population P_S will remain unchanged and be set as *num*. Each individual in P_S will go through state transition operators.

The specific research strategies are as follows.

Step 1 Set the search enforcement of the state transition algorithm as *SE*. The optimal solution search population P_S is evenly generated under random initialization, and the number of the population is set as *num*. Meanwhile, initialize the search in the intermediate population $P_I = 0$, $P_J = 0$, and the Pareto set population P_B.

Step 2 Each individual in P_S will go through state transition operators. The specific operations for each individual of $P_S(i)$ are given as follows:

$best \leftarrow Expansion(P_S(i), SE, \beta, \gamma)$

$best \leftarrow Rotation(P_S(i), SE, \alpha, \beta)$

$best \leftarrow Axesion(P_S(i), SE, \beta, \delta)$

Next, we describe the operator search in detail, taking the expansion operator as an example:

(1) Make *SE* copies of $P_S(i)$ and carry out an expansion operation for each individual; the result is *newpop*
(2) Calculate the fitness value of each individual of *newpop* and make a Pareto non-dominated ranking of $[newpop, P_S(i)]$; and the individuals sorted as 1 are put into the intermediate population P_I. Assign the value of a random Pareto solution to *best*.
(3) $x_{k-1} \leftarrow P_S(i)$, $x_k \leftarrow best$; make *SE* copies of $P_S(i)$ and *best*, and carry out a translation operation for each individual; the result is *newpop* 1.
(4) Calculate the fitness value of each individual of *newpop* 1 and carry out a Pareto non-dominated ranking of $[newpop1, P_S(i)]$; the individuals sorted as 1 are put into an intermediate population P_I. Assign the value of a random Pareto solution to *best*.

Step 3 Perform a state transition operation for all individuals in P_S, and combine the result P_I, P_J with P_B to obtain an intermediate population P_M by Pareto non-dominated ranking. Reassign values to P_S and P_B: assign the first *num* individuals of P_M to P_S, then $P_S = P_M(1 : num)$; put P_{M1}, the individual set with 1 Pareto degree in P_M into P_B, and set $P_I = 0$, $P_J = 0$, $P_M = 0$. If the iteration does not terminate, go to Step 2 for searching.

Improvement of STA operators

In the actual optimization process, when the values of all variables are close to 0, the rotation operator will fall into a potential well. For example, if $x(k) = [0,0]$, doing a search simulation of the rotation operator, if $\alpha = 1$, after doing 10^5 times repetitive search, we obtain the value of $x(k+1)$ shown in Figure 3a (here, a circle shows $x(k+1)$, the result of every search of point $x(k)$).

To overcome these shortcomings, the improvement of operators is done as follows:

$$x_{k+1} = x_k + \alpha \frac{1}{n\|x_k\|_2} R_r(x_k + \varphi) \tag{33}$$

where φ is a smaller positive constant. It has been verified that if $\varphi = 0.0001$, it is able to jump out of the potential well shown in Figure 3b (the black circle represents point $x(k)$, and black dots represent $x(k+1)$, the result of every search).

As shown in the Basic STA, the translation operator only searches along $x(k) - x(k-1)$ in the positive direction. To improve the search ability of the translation operator, we expand the value of $R_t \in R^{n \times n}$ from [0,1] to [−1,1], and make it a bidirectional search range along the axis. The search range of the improved transition algorithm is shown in Figures 4a–b.

Introduction of mutation operator

To avoid the STA algorithm falling into a local optimum in the multiple population search process, we introduce a mutation operator in the section, as shown in Equation (34).

$$x_{k+1} = x_k + R_{ce} randi(Lp - x_k, Up - x_k) \tag{34}$$

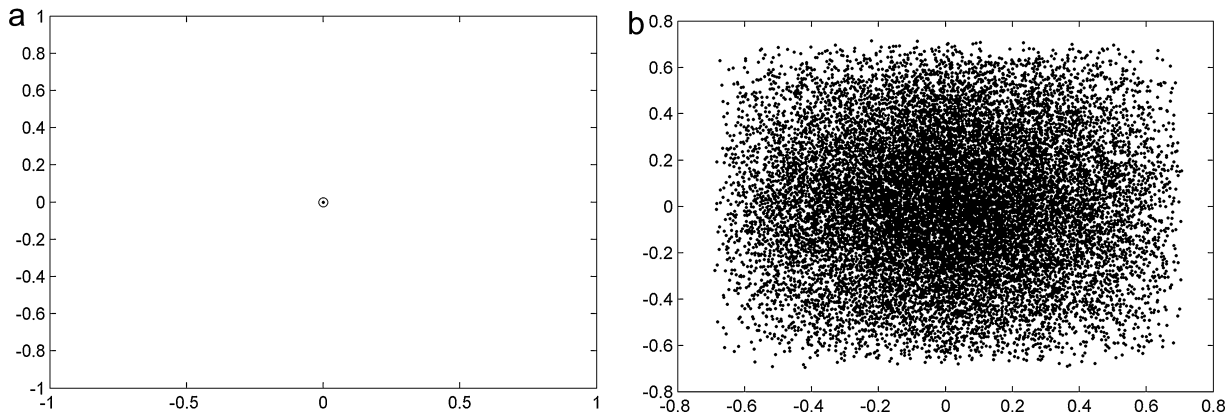

Figure 3. (a) Rotation operator falling into a local potential well. (b) Improved rotation operator search range.

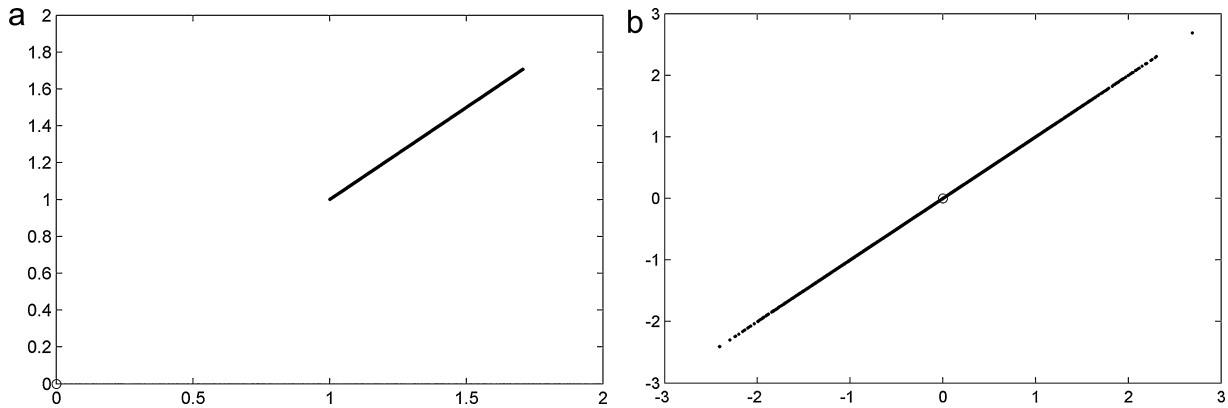

Figure 4. (a) Unidirectional search of translation operator. (b) Bidirectional search of translation operator.

where $R_{ce} \in R^{n\times 1}$ is a vector with its elements obeying a uniform distribution in the range of [0, 1]. *Lp*, *Up* are the lower and upper bounds of the variable value, respectively. $Lp - x_k$ is the expansion towards the lower bound, taking x_k as a starting point. $Up - x_k$ is the expansion towards the upper bound. *randi* is the random expansion towards the lower or upper bounds. The mutation operator will be able to randomly search in the whole domain of definition. To avoid slowing down the search due to excessive mutation, set the number of iterative times of the mutation operator to be divisible by 50; if individuals of the k^{th} generation population P_S and the $\text{k}+1^{\text{th}}$ generation population P_S are the same, execute the mutation operator.

MOSTA with Constraint Handling Strategy for CMOP

The space S of the constrained multi-objective optimization problem (CMOP) can be divided into the feasible solution space (denoted as Ω) and the infeasible solution space (denoted as Z), as shown in Figure 5, where $x_i\,(i=1,2,3,4)$ is the feasible solution and $y_i\,(i=1,2,3,4)$ is the infeasible solution. Assume that x^* is the global optimal solution and y_1 is the closest one to x^*. If the infeasible solution y_1 is not excluded by the algorithm, it may explore the boundary regions from new directions where the optimum is likely to be found. It is necessary for CMOP to properly use its infeasible solutions.

Constraint handling strategy based on the multi-objective method

As mentioned in the Introduction section, researchers have gradually realized the merit of infeasible solutions in searching for the global optimum in the feasible region by trying to save and utilize those infeasible solutions with better performances.[48] Lin[49] formulated an adaptive evolutionary strategy to ensure that infeasible solutions with slight violations can be reserved with the adaptive proportion of the population to find optimal solutions from all possible directions. Based on this idea, we propose a constraint handling strategy based on the multi-objective method, which is a novel infeasible solution replacement mechanism that saves infeasible solutions with better performance and allows them to participate randomly in the subsequent evolution, so as to avoid constructing a penalty function and deleting meaningful infeasible solutions directly.

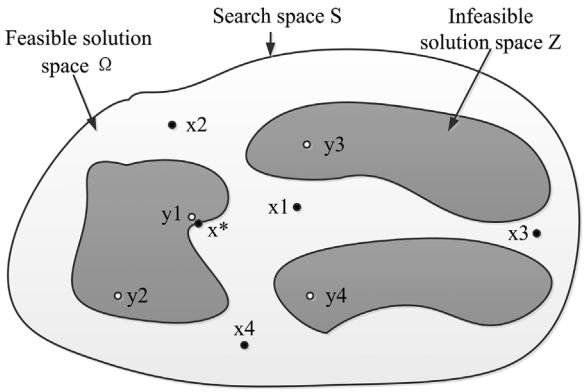

Figure 5. Distribution diagram of the search space.

The detailed description of the constraint handling strategy is as follows. For the optimization problem of Equation (32), we reconstruct an unconstrained optimization problem with two types of objectives. The first type of objectives is objective $F(X)$ in the original problem, and the other is the constraint violation degree of individual $G(X)$. First, equality constraints are transformed into inequality constraints as $|h_j(X)| - \mu \leq 0$, where $j = p+1, ..., q$ and μ is a positive tolerance value. Hence, the constraint violation degree of individual X on the i^{th} constraint is calculated as follows.

$$G_i(X) = \begin{cases} \max\{0, g_i(x)\}, \ (i = 1, 2, ..., p) \\ \max\{0, |h_i(x)| - \mu\}, \ (i = p+1, ..., q) \end{cases} \tag{35}$$

Then, the individual violation degree of all constraint conditions is $G(X)$:

$$G(X) = \sum_{i=1}^{q} G_i(X) \tag{36}$$

If $G(X) = 0$, it means that the individual is a feasible solution satisfying all of the constraint conditions. If $G(X) > 0$, the individual is an infeasible solution. The larger $G(X)$ is, the larger the individual violation degree will be.

Due to the constraints having different properties in type, dimension, and characteristics, we need to standardize the violation degree of every constraint and obtain Equation (37):

$$\tilde{G}(X) = \frac{1}{q} \times \sum_{i=1}^{q} \frac{G_i(X)}{G_{i\max}} \tag{37}$$

where $G_{i\,max}$ is the maximum value of the violation degree of the i^{th} constraint, and q is the total number of constraints.

To take advantage of the infeasible solutions with better performances, we adaptively determine the proportion of the infeasible solutions to be reserved and save the iterative solutions according to the following rules.

1) Among two feasible solutions $\vec{X}$, $\vec{X}'$, the one that has a better objective function value $\tilde{G}(X)$ is preferred
2) Among two infeasible solutions $\vec{X}$, $\vec{X}'$, the one that has a smaller degree of constraint violation $\tilde{G}(X)$ is preferred
3) Assume that $\vec{X}$ is a feasible solution and $\vec{X}'$ is an infeasible solution; if $\tilde{G}(\vec{X}') \leq \varepsilon$, then $F(\vec{X}'') < F(X)$, $\vec{X}''$will $\vec{X}'$ be preferred. Otherwise, $\vec{X}$ will be preferred

where ε is the threshold of the constraint violation degree. The larger the value of ε, the higher the proportion of the infeasible solution in the optimal solution.

To maintain the proportion p_c of the infeasible solution, the value of ε is adjusted adaptively according to the following formula.

$$\varepsilon' = \begin{cases} 1.2 * \varepsilon, \ P_K < P_C \\ 0.8 * \varepsilon, \ P_K > P_C \\ \varepsilon, \qquad Other \end{cases} \tag{38}$$

where p_k is the average proportion of the infeasible solution for each K generations during the evolution process.

$$p_k = \left(\sum_{i=k*K+1}^{k*K+K} N_i \right) \Big/ (K \times num), k = 0, 1, 2, ..., n \tag{39}$$

where N_i is the number of infeasible solutions in the i^{th} generation, and num is the number of the population in each generation.

The proposed constraint handling strategy can be applied to solve the COPs well to ensure searching for the optimal solutions continuously.

Framework of the proposed hybrid algorithm

To solve CMOP in AEP, the above proposed constraint handling strategy is integrated into MOSTA. The integration makes MOSTA come out with multiple groups of functional partitions. These partitions include an evolutionary population P_S of size num, an intermediate population P_I of size $num1$ to save feasible individuals, an intermediate population P_J of size $num2$ to save infeasible individuals, a population P_B to save the optimal feasible solution found in the search process, an intermediate population P_M of size $num3$ to save the best individuals from P_I, and an intermediate population$P_{M1}$of size $num3$ to save the best individuals from P_J to select optimal solutions from all possible directions. The relationship of the multi-population is shown in Figure 6.

The detailed description of the proposed algorithm follows.

Step 1 (Initialization). Generate the populations P_S, P_B, P_I, P_J, P_M, and P_{M1}, then set the values of $G_{\max}$ (the number of function evaluations), K (the generation of evaluation by adaptive fix the value of ε), num (population size), SE (the number of search population individuals), ε (the maximum constraint violation degree), $g = 1$ (the current generation number), and α, β, γ, δ (operation index). Randomly generate the parent population P_S of size pop from the decision space, set the P_B, and let the intermediate populations P_I and P_J be empty.

Step 2 (Mutation Operator). If the number of iterations is divisible by 50, and the k^{th} generation P_S are the same as the $k+1^{\text{th}}$ generation P_S, the mutation of the parent optimal population P_S can be obtained by executing the mutation operator. Otherwise, go to Step 3 directly.

Step 3 (Strategy of MOSTA). For every individual of population P_S, we carry out the STA. Here, the improvement of the rotation operator and translation operator will be used from the Improved STA operators section. For every individual of $P_S(i)$ carry out the search strategy in the Archive Strategy of Multi-population section, and then we can obtain the intermediate population P_I and P_J.

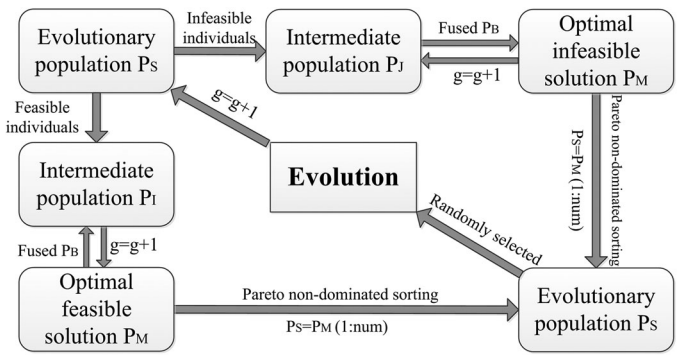

Figure 6. Relationship diagram of multi-population.

Step 4 (Strategy of CMOSTA). To calculate the individual violation degree of the intermediate population in the Archive Strategy of Multi-population section, the feasible and infeasible solutions will be non-dominated ranked by the constraint handling strategy, and we obtain the new intermediate populations P_M and P_{M1}.

Step 5 (evolution or termination). If $g < G_{\max}$, then $g = g + 1$, and go to Step 2. Otherwise, make the best population P_B part of the Pareto optimization set P^*, and output P^*.

ALGORITHM SIMULATION AND ANALYSIS

Example Validation

Evaluation criteria

Unlike single-objective optimization, solution quality evaluation in the case of multi-objective optimization is more complicated. Criteria to evaluate multi-objective optimization algorithms can be categorized as two types: evaluating the convergence degree by computing the proximity between the solution frontier and the actual Pareto frontier; and evaluating the distribution degree of the solutions in the objective space by computing the distances between the individuals. Here, we choose both criteria to evaluate the performance of the CMOSTA.

(1) Convergence Evaluation *CE*: The extent of convergence to a known Pareto optimal set.[18]

$$CE = \frac{1}{Q}\left(\sum_{i=1}^{Q} \min \|P^* - P_{FT}\|\right) \tag{40}$$

where P^* is the obtained non-domination Pareto frontier, P_{FT} is the real non-domination Pareto frontier, $\|P^* - P_{FT}\|$ is the Euclidean distance of P^* with P_{FT}, and Q represents is the number of obtained solutions.

(2) Distribution Degree Evaluation: The non-uniformity in the distribution is measured by *SP* as follows:[18]

$$SP = \sqrt{\frac{1}{(Q-1)} \sum_{i=1}^{Q} \left(\bar{d} - d_i\right)^2} \tag{41}$$

where d_i represents the Euclidean distance among consecutive solutions in the obtained non-dominated set of solutions and parameter $\bar{d}$ is the average distance.

Experimental study

In this section, we choose four problems, CTP1, SRN, TNK, and BNH, to test the proposed method, as shown in Table 1. We compare the method with the classic NSGA-II.[18]

The simulation environment was an Intel Pentium 4, 3.06 GHz CPU, 4 GB Memory, Windows XP Professional, Matlab 7.1. The parameters are initialized as follows: the size of population P_S is $num = 100$, number of search population $SE = 10$ maximum evolution generation $G_{\max} = 200$, and crossover operator is 20, $\alpha = 1$, $\beta = 1$, $\gamma = 1$, $\delta = 1$. The adaptive generation of evaluation is $K = 5$, maximum of constraint violation degree $\varepsilon = 0.8$, NSGA-II population size $pop_1 = 100$, maximum evolution generation $G_{\max 1} = 200$, and crossover operator setting is 20. Each algorithm runs 20 times independently for each test function.

Figures 7a–d are comparison charts between the proposed algorithm and NSGA-II after a random running of the four test

Table 1. Test function

Test Function	Objective Function min $F(X) = \min[f_1(X), f_2(X)]$	Constraint	Range of Variable
CTP1	$f_1(X) = x_1$; $f_2(X) = \exp\left(-\frac{f_1(X)}{c(X)}\right) \times \left\{41 + \sum_{i=2}^{5}[x_i^2 - 10\cos(2\pi x_i)]\right\}$.	$g_1(X) = \cos(\theta)(f_2(X) - e) - \sin(\theta) f_1(X)$; $g_2(X) = a\left\lvert \sin\left\{ b\pi[\sin(\theta)(f_2(X) - e) + \cos(\theta) f_1(X)]^c \right\} \right\rvert^d$; $g_1(X) \geq g_2(X)$.	$0 \leq x_1 \leq 1$ $-5 \leq x_1 \leq 5\ i = 2, 3, 4, 5$
SRN	$f_1(X) = 2 + (x_1 - 2)^2 + (x_2 - 1)^2$; $f_2(X) = 9x_1 - (x_2 - 1)^2$.	$g_1(X) = x_1^2 + x_2^2$; $g_2(X) = x_1 - 3x_2 + 10$; $g_1(X) - 225 \leq 0$; $g_2(X) \leq 0$.	$-20 \leq x_1 \leq 20$ $-20 \leq x_2 \leq 20$
BNH	$f_1(X) = 4x_1^2 + 4x_2^2$; $f_2(X) = (x_1 - 5)^2 + (x_2 - 5)^2$.	$g_1(X) = (x_1 - 5)^2 + x_2^2 - 25$; $g_2(X) = -(x_1 - 8) + (x_2 + 3) + 7.7$; $g_1(X) \leq 0$; $g_2(X) \leq 0$.	$0 \leq x_1 \leq 5$ $0 \leq x_2 \leq 3$
TNK	$f_1(X) = x_1$; $f_2(X) = x_2$.	$g_1(X) = -x_1^2 - x_2^2 + 1 + 0.1\cos(16\arctan(x_1/x_2))$; $g_2(X) = (x_1 - 0.5)^2 + (x_2 - 0.5)$; $g_1(X) \leq 0$; $g_2(X) - 0.5 \leq 0$.	$0 \leq x_i \leq \pi\ i = 1, 2$

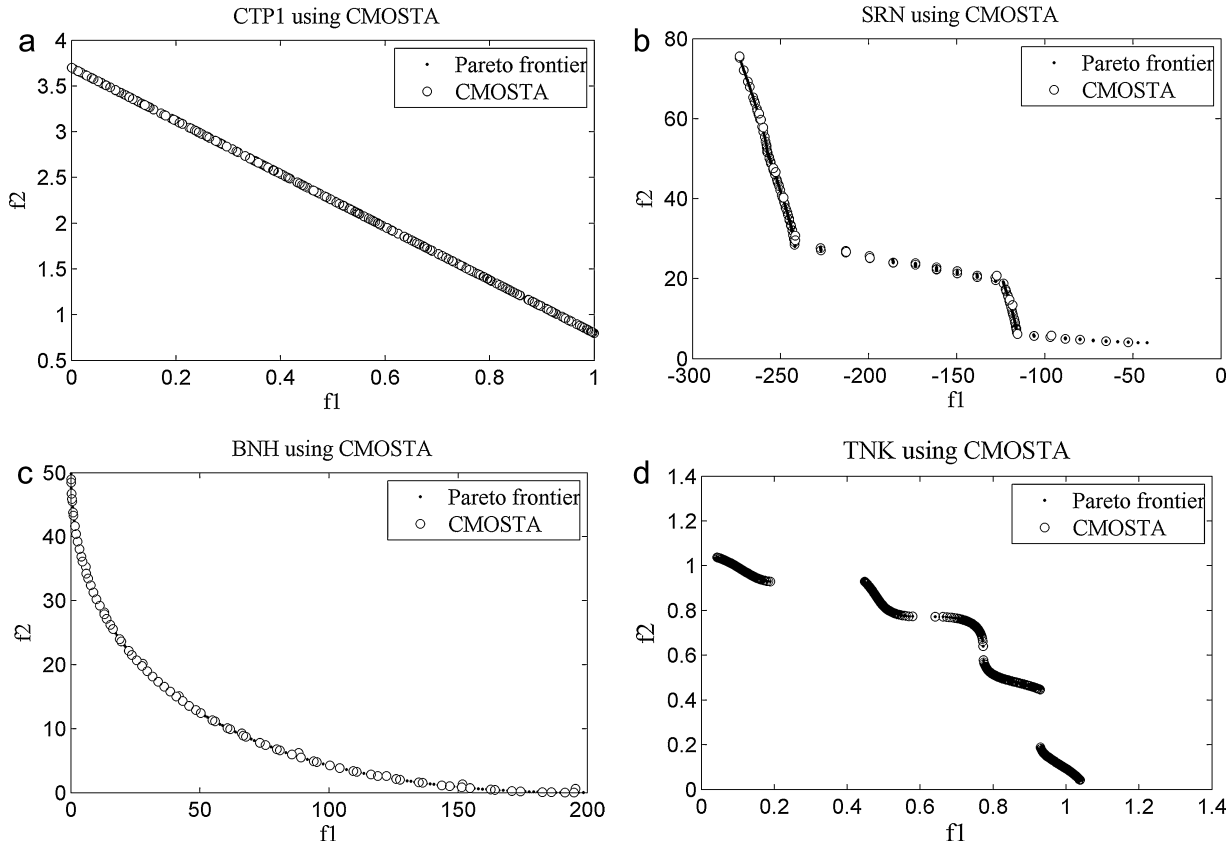

Figure 7. (a–d) Comparison charts of Pareto frontier.

functions. '○' are the optimal solutions given by CMOSTA, and '•' is the true Pareto frontier. It is obvious that the proposed algorithm returns a better approximation of the true Pareto-optimal frontier and a distribution of higher uniformity. We also evaluated algorithms based on the two criterions *CE* and *SP*. It can be observed from the data in Table 2 that the proposed algorithm performs significantly better than the classical NSGA-II algorithm in convergence and distribution uniformity. Simulation results show that this algorithm can accurately converge to global Pareto solutions and can maintain population diversity.

Industrial Numerical Experiments

In this section, we use industry data of actual AEP to solve the operating parameters of the optimization model with the CMOSTA so as to verify its validity.

The operating parameters are initialized as follows. The heat transfer areas of the first to third evaporators are $S_i = 1230\,\mathrm{m}^2$ $(i = 4,5,6)$; the fourth evaporator is $S_7 = 1600\,\mathrm{m}^2$; the range of the condenser pressure is $P_m \in [0.01\,\mathrm{MPa},\ 0.03\,\mathrm{MPa}]$; the pressure of live steam is $P_0 \in [0.4\,\mathrm{MPa},\ 0.6\,\mathrm{MPa}]$; the heat transfer coefficients of the four evaporators are $Q_i = 849.7\,\mathrm{W/m^2 \cdot K}$, $2025\,\mathrm{W/m^2 \cdot K}$, $829.7\,\mathrm{W/m^2 \cdot K}$, $721.8\,\mathrm{W/m^2 \cdot K}$ $(i = 4, 5, 6, 7)$. Flow limitation of the feed mother liquor flowed into the IIIrd evaporator is 0–30 t/h, the concentration of the mother liquor output $X_{out} \in [160\,\mathrm{g/L},\ 170\,\mathrm{g/L}]$, and the concentration of feed mother liquor is 87 g/L. The same parameters of CMOSTA are omitted here.

Figure 8 is the Pareto frontier of the CMOSTA after running 50 times; the optimal parameters of the evaporation process are listed in Table 3 (AV is actual practice value, and OR is optimal value of algorithm); the distribution of optimal temperature differences in the evaporation process can be represented by a

Table 2. Performance comparison

Test Function	Algorithm	*CE*	*SP*
CTP1	NSGA-II	$0.021\,317 \pm 0.000\,323$	$0.873\,321 \pm 0.087\,25$
	CMOSTA	$0.014\,585 \pm 0.000\,261$	$0.682\,149 \pm 0.025\,63$
SRN	NSGA-II	$0.011\,120 \pm 0.000\,753$	$0.783\,14 \pm 0.028\,43$
	CMOSTA	$0.009\,501 \pm 0.000\,406$	$0.344\,712 \pm 0.013\,56$
BNH	NSGA-II	$0.014\,947 \pm 0.000\,632$	$0.336\,941 \pm 0.009\,17$
	CMOSTA	$0.012\,857 \pm 0.000\,231$	$0.187\,919 \pm 0.007\,18$
TNK	NSGA-II	$0.013\,235 \pm 0.000\,740$	$0.464\,542 \pm 0.007\,30$
	CMOSTA	$0.008\,913 \pm 0.000\,168$	$0.173\,482 \pm 0.003\,76$

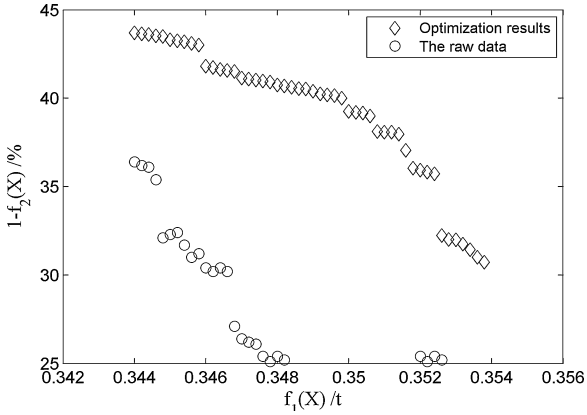

Figure 8. Pareto frontier of CMOSTA optimization.

function of optimal outlet mother liquor concentration. Combined with true output data, outlet concentrations of the mother liquor in every unit obtained by optimization and calculation are shown in Table 4. It should be noted that the optimal solution obtained is just the best solution from industrial numerical experiments so far, since the real Pareto frontier in AEP is unknown under the conditions of actual alumina production process.

The results show that the exergy efficient and J_1 conflict. If we want to improve the exergy efficiency, J_1 must be reduced. However, these two conflicting objectives are measured by the Pareto dominance relation, and they maintain a balance under the Pareto optimality criterion. The optimal solution shows that the outlet mother liquor concentration coming from the #1 flash evaporator satisfying concentration requirements of subsequent process is up to 160 g/L. Similarly, the energy loss efficiency decreases by about 13.39 % compared to the actual results, as we reduced the mass of live steam used to evaporate each tonne of water by about 13.63 %. Similarly, when the concentration of final mother liquor satisfied the requirements, the mass of live steam used to evaporate each tonne of water was reduced by about 6.16 %. Therefore, the qualification rate of mother liquor has been improved, which is beneficial to energy saving and emission reduction of the evaporation process.

Results over 23 days are shown in Figure 9. Comparing VMPSO optimal results with those of CMOSTA, the live steam flow of CMOSTA optimization is reduced with an average of about 0.167 t. Comparing the results obtained by COMSTA with actual results, the live steam flow is also reduced with an average of about 0.625 t, which indicates that CMOSTA has better performance than VMPSO.

CONCLUSIONS

To further save energy and reduce consumption, optimization of both the operating costs and energy consumption of AEP were studied in this paper. By introducing the index of exergy evaluation, we have established an optimization model to maintain the balance between operating costs and energy efficiency while satisfying the concentration requirement of the final mother liquor. As for the complex multiple-objective optimization problem with constraints, we have proposed a multi-objective state transition algorithm with a few beneficial features in which an archiving mechanism and an infeasible solution replacement mechanism based on multi-objective optimization are integrated to find optimal solutions from all possible directions. Moreover, the new state transition operator and mutation operator are introduced, which aim to direct the population to approach or land in the feasible region from different directions during the evolutionary process. Simulation results on benchmarks and industrial applications indicate that the proposed algorithm can converge quickly and effectively to the true Pareto frontier with better distribution, which is helpful to inspire further research on evolutionary methods for engineering optimization.

Table 3. Optimal parameters and production index of the AEP

Item	P_0 (MPa)	F_{01} (m^3/h)	Δt_4 (°C)	Δt_5 (°C)	Δt_6 (°C)	Δt_7 (°C)	J_1 (t)
AV	0.58	258.035	30.08	10.43	27.97	19.34	0.402
OR							
VMPSO	0.453	0.00	31.68	10.86	25.87	16.38	0.370
CMOSTA	0.446	0.00	30.02	13.89	25.41	17.39	0.3472
Item	P_m (MPa)	T_0 (K)	V_0 (t)		V_1 (t/h)	η_t (%)	f_2 (%)
AV	0.020	339.71	61.17	163.94	59.32	28.40	71.60
OR							
VMPSO	0.012	342.95	52.42	169.95	52.42	–	–
CMOSTA	0.016	345.92	50.33	160.51	51.48	41.79	58.21

Table 4. Unit concentration of output mother liquor under most-efficiency operations

Unit	C_1^2 (g/L)	C_2^2 (g/L)	C_3^2 (g/L)	C_4^2 (g/L)	C_5^2 (g/L)	C_6^2 (g/L)	C_7^2 (g/L)
AV	163.94	160.7	156.78	155.7	125.47	110.93	98.49
OR	160.51	159.92	156.41	153.92	124.7	108.84	96.54

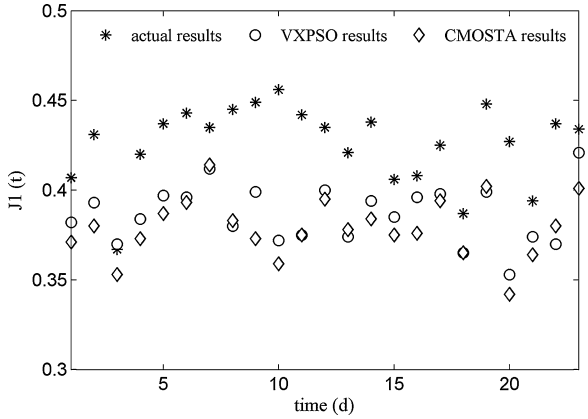

Figure 9. Comparisons of live steam flow.

ACKNOWLEDGEMENTS

This waork is supported by the National Natural Science Foundation of China (Grant No. 61273187 and 61503416), the Innovation-drive Plan in Central South University (Grant No. 2015cx007), and the National High Technology Research and Development Program of China (863 Program) (Grant No. 2014AA041803).

NOMENCLATURE

C_i^i	concentration of sodium carbonate components, sodium hydroxide components, and alumina components respectively from the *j*th component to the *i*th evaporator (kg/m^3)
cp_i	specific heat capacity of mother liquor output from the *i*th unit (KJ/kg · K)
c_i	specific heat capacity of mother liquor from the *i*th unit (KJ/kg · K)
c_{out}	specific heat capacity of final mother liquor (KJ/kg · K)
c_w	specific heat capacity of water (KJ/kg · K)
D_0	total quantity of live steam (kg)
e_{coi}	exergy of flash steam from condensate to the sixth unit (J/kg)
e_{mi}	exergy of the mother liquor output from the *i*th unit (J/kg)
e_{mpi}	exergy of the mother liquor output from the *i*th preheater unit (J/kg)
e_{ni}	exergy of the mother liquor output from the *i*th evaporator unit (J/kg)
e_{vi}	exergy of per mass vapour from the *i*th unit (J/kg)
e_{v0}	exergy of live steam (J/kg)
F_i	flow of feed mother liquor put into the *i*th unit (m^3/h)
F_{01}	flow of mother liquor put into the 6th unit (m^3/h)
H_{is}	enthalpy of live steam from the *i*th flash evaporator to evaporator (kJ/kg)
H_r	enthalpy of water output under (T_r,p_r) condition (kJ/kg)
H_{out}	enthalpy of water output under (t_{out}, p_{out}) condition (kJ/kg)
H_i	specific enthalpy of steam from the *i*th units under live steam and P_0 conditions (kJ/kg)
h_i	latent heat of vapour output from the *i*th unit (kJ/kg)
h_0	latent heat of live steam (kJ/kg)
J_1	operating cost function
k_i	heat transfer coefficient of the (*i*-3)th evaporator (W/m^2 · K)
P_m	condenser pressure (MPa)
P_0	live steam pressure (MPa)
P_{m0}	pressure of feed mother liquor (MPa)
P_{mi}	pressure of mother liquor from the *i*th unit (MPa)
P_{out}	pressure of final mother liquor (MPa)
Q_i	heat load of the *i*th evaporator (MPa)
S_i	heat transfer area of the *i*th evaporator (m^2)
s_{m0}	specific entropy of water output under the (t_{m0},p_{m0}) condition (J/mol)
s_{out}	specific entropy of water output under the (t_{out},p_{out}) condition (J/mol)
s_r	specific entropy of water output under the (T_r,p_r) condition (J/mol)
s_{ni}	specific entropy of the *i*th evaporator under vapour pressure and T_{ni} conditions (J/(K · kg)
s_{wi}	specific entropy of the *i*th evaporator under condensate pressure and T_{wi} conditions (J/(K · kg)
s_i	specific entropy of steam units under live steam and P_0 conditions (J/mol)
T_0	temperature of feed mother liquor (K)
T_{ni}	temperature of vapour outlet from the *i*th unit (K)
T_{wi}	temperature of flash steam outlet from the *i*th unit (K)
t_{oi}	temperature of mother liquor outlet from the *i*th unit (K)
T_r	absolute zero temperature (273 K)
Δt_i	effective temperature difference of the *i*th evaporator (K)
T_{isf}	temperature of the $i^{\#}$ flash steam (K)
T_{is}	temperature of live steam from the *i*th flash evaporator to evaporator
t_{mi}	temperature of mother liquor outlet from the *i*th unit (K)
t_{out}	temperature of final mother liquor outlet (K)
V_0	flow of initial live steam (kg/h)
V_i	flow of vapour steam output from the ith unit (kg/h)
V_{is}	flow of live steam from the *i*th flash evaporator to evaporator
$V_{i,max}$	maximum velocity of live steam from the ith evaporator (m^3/h)
$V_{i,min}$	minimum velocity of live steam from the ith evaporator (m^3/h)
v_w	specific volume of water (m^3/kg)
v_{m0}	specific volume of liquid (m^3/kg)
v_{mi}	specific volume of mother liquor output from the *i*th unit (m^3/kg)
v_{out}	specific volume of final mother liquor outlet (m^3/kg)
W	total quantity of water evaporated from the mother liquor (kg)
ρ_0	density of feed mother liquor (kg/m^3)
ρ_i	density of mother liquor output from the *i*th unit (kg/m^3)
η_t	exergy efficiency
η_e	total exergy loss of AEP
η_{exi}	exergy loss from internal heat transfer in AEP
η_{exo}	exergy loss from external heat transfer in AEP

REFERENCES

[1] Z. Chen, H. Chen, *World Nonferrous Metals* **2004**, *4*, 41.

[2] H. Zhu, Q. Chai, C. Yang, X. Wang, *Can. J. Chem. Eng.* **2012**, *90*, 1418.

[3] L. Liu, Z. Lu, Q. Yu, S. Yan, Y. Jiang, Z. Lu, *Chinese J. Nonfer. Met*. **2002**, *12*, 1294.

[4] X. Ji, J. Lundgren, C. Wang, J. Dahl, *Appl. Energ*. **2012**, *97*, 30.

[5] S. Khanam, B. Mohanty, *Appl. Energ*. **2010**, *87*, 1102.

[6] H. Heluane, M. Colombo, M. R. Hernández, M. Graells, L. Puigjaner, *Chem. Eng. Process*. **2007**, *46*, 198.

[7] Q. Chai, C. Yang, K. L. Teo, W. Gui, *Control. Eng. Pract*. **2012**, *20*, 618.

[8] J. D. Schaffer, "Multiple objective optimization with vector evaluated genetic algorithms," in *Proceedings of the 1st international Conference on Genetic Algorithms*, Morgan Kaufmann Publishers, Hillsdale, NJ, USA **1985**, p. 93.

[9] K. Deb, *Multi-objective optimization using evolutionary algorithms*, 1st edition, John Wiley & Sons, Weinheim **2001**, p. 81.

[10] C. A. C. Coello, G. B. Lamont, D. A. Van Veldhuizen, *Evolutionary algorithms for solving multi-objective problems*, 2nd edition, Springer, New York **2007**, p. 61.

[11] C. A. C. Coello, G. B. Lamont, *Applications of multi-objective evolutionary algorithms*, 1st edition, World Scientific, Singapore **2004**, p. 6.

[12] B. J. Ritzel, J. W. Eheart, S. Ranjithan, *Water. Resour. Res*. **1994**, *30*, 1589.

[13] K. Miettinen, *Nonlinear multi-objective optimization*, 1st edition, Kluwer Academic Publishers, Norwell, MA, USA **1999**, p. 115.

[14] L. Tang, X. Wang, *IEEE T. Evolut. Comput*. **2013**, *17*, 20.

[15] C. M. Fonseca, P. J. Fleming, "Genetic Algorithms for Multiobjective Optimization: Formulation, Discussion and Generalization," *Proceedings of the 5th International Conference on Genetic Algorithms*, Morgan Kaufmann Publishers, Urbana-Champaign, IL, USA, 6–13 June **1993**, p. 416.

[16] J Horn, N Nafpliotis, D. E. Goldberg, "A niched Pareto genetic algorithm for multi-objective optimization," *Proceedings of the 1st IEEE Conference on Evolutionary Computation*, IEEE Computer Society, Orlando, FL, USA, 27–29 June **1994**, p. 82.

[17] N. Srinivas, K. Deb, *Evol. Comput*. **1994**, *2*, 221.

[18] K. Deb, A. Pratap, S. Agarwal, T. Meyarivan, *IEEE T. Evolut. Comput*. **2002**, *6*, 182.

[19] C. A. C. Coello, G. T. Pulido, "A micro-genetic algorithm for multi-objective optimization," *Proceedings of the Genetic and Evolutionary Computation Conference (GECCO)*, Morgan Kaufmann Publishers, San Francisco, USA, 7–11 July **2001**, p. 274.

[20] J. D. Knowles, D. W. Corne, *Evol. Comput*. **2000**, *8*, 149.

[21] E. Zitzler, L. Thiele, *IEEE T. Evolut. Comput*. **1999**, *3*, 257.

[22] E. Zitzler, M. Laumanns, L. Thiele, "SPEA2: Improving the strength Pareto evolutionary algorithm," in *Evolutionary Methods for Design, Optimization and Control with Applications to Industrial Problems*, Springer, Athens, Greece **2001**, p. 95.

[23] K. C. Tan, T. H. Lee, E. F. Khor, *IEEE T. Evolut. Comput*. **2001**, *5*, 565.

[24] Q. Zhang, H. Li, *IEEE T. Evolut. Comput*. **2007**, *11*, 712.

[25] H. Li, Q. Zhang, *IEEE T. Evolut. Comput*. **2009**, *13*, 284.

[26] R. P. Beausoleil, *Eur. J. Oper. Res*. **2006**, *169*, 426.

[27] A. J. Nebro, F. Luna, E. Alba, B. Dorronsoro, J. J. Durillo, A. Beham, *IEEE T. Evolut. Comput*. **2008**, *12*, 439.

[28] C. A. C. Coello, G. T. Pulido, M. S. Lechuga, *IEEE T. Evolut. Comput*. **2004**, *8*, 256.

[29] C. K. Goh, K. C. Tan, D. S. Liu, S. C. Chaim, *Eur. J. Oper. Res*. **2010**, *202*, 42.

[30] B. Surekha, L. K. Kaushik, A. K. Panduy, P. R. Vundavilli, M. B. Parappagoudar, *Int. J. Adv. Manuf. Tech*. **2012**, *58*, 9.

[31] W. Y. Gong, Z. H. Cai, *Eur. J. Oper. Res*. **2009**, *198*, 576.

[32] Y. Wang, X. Chen, W. Gui, C. Yang, L. Caccetta, H. Xu, *J. Appl. Math*. **2013**, DOI:10.1155/2013/841780

[33] A. Al-Ani, A. Alsukker, R. N. Khushaba, *Swarm. Evolut. Comput*. **2013**, *9*, 15.

[34] Z. Michalewicz, M. Schoenauer, *Evol. Comput*. **1996**, *4*, 1.

[35] Z. Michalewicz, K. Deb, M. Schmidt, T. Stidsen, *IEEE T. Evolut. Comput*. **2000**, *4*, 197.

[36] C. A. C. Coello, *Comput. Method. Appl. M*. **2002**, *191*, 1245.

[37] Y. Wang, Z. Cai, *IEEE T. Evolut. Comput*. **2012**, *16*, 117.

[38] K. Deb, *Comput. Method. Appl. M*. **2000**, *186*, 311.

[39] E. Mezura Montes, C. A. C. Coello, *IEEE T. Evolut. Comput*. **2005**, *9*, 1.

[40] X. Zhou, C. Yang, W. Gui, "Initial version of state transition algorithm," *Proceedings of the 2th International Conference on Digital Manufacturing and Automation (ICDMA)*, IEEE Computer Society, Zhangjiajie, China, 5–7 August **2011**, p. 644.

[41] D. R. Morris, J. Szargut, *Energy* **1986**, *11*, 733.

[42] W. Wagner, *Extended IAPWS-IF97 Steam Tables: Interactive Software for the Calculation of Thermodynamic and Transport Properties of Water and Steam-DLL for User Specific Programs*, 2nd edition, Springer, New York **2006**, p. 11.

[43] H. Chang, J. Li, *Chem. Eng. Sci*. **2005**, *60*, 2771.

[44] X. Zhou, C. Yang, W. Gui, *J. Ind. Manag. Optim*. **2012**, *8*, 1039.

[45] X. Zhou, D. Gao, C. Yang, *Adv. Intel. Syst. Comput*. **2013**, *212*, 651.

[46] C. Yang, X. Tang, X. Zhou, *Control. Theory. A* **2013**, *30*, 1040.

[47] X. Zhou, C. Yang, W. Gui, *Appl. Math. Comput*. **2014**, *226*, 169.

[48] Y. Wang, Z. Cai, *IEEE T. Evolut. Comput*. **2012**, *42*, 203.

[49] D. Lin, M. Q. Li, J. S. Kou, *J. Software* **2001**, *12*, 628.

Manuscript received January 30, 2015; revised manuscript received March 17, 2015; accepted for publication April 9, 2015.